P8.17

HYDROLOGICAL PARAMETERS DERIVED FROM AQUA AMSR-E MEASUREMENTS

Banghua Yan[1*] and Fuzhong Weng[2]

[1]QSS Group Inc, Camp Springs, Maryland
[2]NOAA/NESDIS/ORA/JCSDA, Camp Springs, Maryland

1. INTRODUCTION

The ability of microwave satellite-measurements at relatively high frequencies to drive cloud liquid water over oceans has been well recognized [Weng and Grody, 1994; Wentz, 1997; Weng et al., 2003]. However, the brightness temperature at 37 GHz becomes insensitive to cloud liquid water for raining clouds. Thus, previously developed algorithms about cloud liquid water are mostly inapplicable for raining clouds. With Aqua AMSR-E instrument, launched on May 4, 2002, which is a conically scanning passive microwave radiometer at 6 frequencies ranging from 6.9 to 89 GHz with both horizontal and vertical polarization, we can extend our capability to retrieve rain water through uses of lower frequencies. In this paper, a previously-developed emission-based algorithm for cloud liquid water [Weng and Grody, 1994; Weng, et al., 2003] is modified to retrieve the rain water over oceans using AMSR-E measurements at 10.65 and 23.8 GHz. The parameters of sea surface temperature (SST) and wind (SSW) in the rain water algorithm are also derived using AMSR-E measurements at 6.925 and 10.65 GHz.

2. CHARACTERISTICS OF AMSR-E CHANNELS AT LOWER FREQUENCIES OVER OCEANS

AMSR-E instrument provides six frequency measurements at 6.925, 10.65, 18.7, 23.8, 36.5 and 89 GHz with both vertical and horizontal polarization. Its channel characteristics against cloud liquid water, SST and SSW over oceans are evaluated using a vector radiative transfer model [Weng, 1992; Weng and Liu, 2003], as discussed below.

Figure 1 shows simulated brightness temperatures (T_V) against cloud liquid water. Note that the lower frequencies respond to cloud liquid water linearly within a large dynamic range. Several other AMSR-E frequencies are also shown for a condition of SSW of 10 m/s and SST of 300 °K. It is found that when cloud liquid water is small (e.g., in non-raining clouds) 36.5 GHz is the most sensitive channel. However, the measurements at 37 GHz will become saturated and further decreased when cloud liquid water is greater than 1.0 mm. At 10.65 GHz, saturation is about 8 mm which sufficiently covers the dynamic range of cloud liquid water in various raining conditions. It is noted that T_V at 6.925 GHz is least sensitive to cloud liquid water especially over high winds. For example, when SSW = 20 m/s and SST = 281 °K, the variations in T_V at 6.925 is about 4 °K, for a variation of 2 mm (0 to 2 mm) in cloud liquid water. Also horizontally polarized brightness temperatures (T_H) are more strongly affected by wind roughness, as mentioned in [Weng and Grody, 1994]. Thus, in our AMSR-E cloud algorithm, the vertically polarized brightness temperatures at 10.65 and 23 GHz are utilized to retrieve rain water.

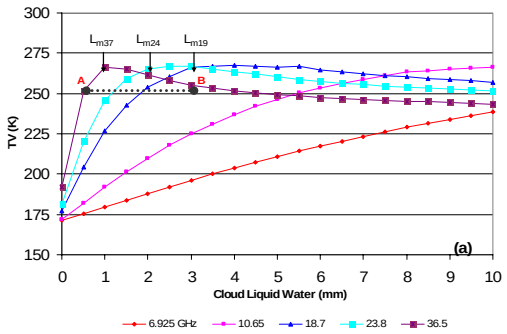

Figure 1. Simulated vertically polarized brightness temperatures (T_V) at 6.925, 10.65, 18.7, 23.8 and 36.5 GHz as a function of cloud liquid water.

Lower frequencies (6.925 and 10.65 GHz) of AMSR-E measurements over oceans are much sensitive to SST and SSW although this sensitivity varies with polarization of brightness temperatures. Figures 2a illustrates T_V at 6.925 and 10.65 GHz as a function of SST under various atmospheric conditions for SSW of 5 and 25 m/s, respectively. It is seen that when SST varies from 282 to 302 °K, the variation of T_V is about 13 °K. For the same conditions, the variation of T_H is only about 8 °K due to lower horizontal ocean emissivity (not shown here). Figure 2b displays simulated T_H at 6.925 and 10.65 GHz as a function of SSW for various atmospheric profiles.

---

* Corresponding author address: *Dr. Banghua Yan, JCSDA, NOAA/NESDIS/ORA, 5200 Auth Road, Room 810, Camp Springs, MD 20746,; email: banghua.yan@noaa.gov*

When SSW varies from 1 to 50 m/s, the variation in T_H is up to 45°K. For the same conditions, the variation in T_V is up to 7 °K (not shown here). Thus, in following AMSR-E surface algorithm for SST and SSW, all of T_V and T_H at 6.925 and 10.65 GHz are utilized. As illustrated in Fig. 1 above, the polarized brightness temperatures at 10.65 GHz are also sensitive to cloud liquid water. Thus, the atmospheric transmittance and upwelling (downwelling) radiance are treated as retrieval variables in the AMSR-E surface algorithm (see section 3.2 below).

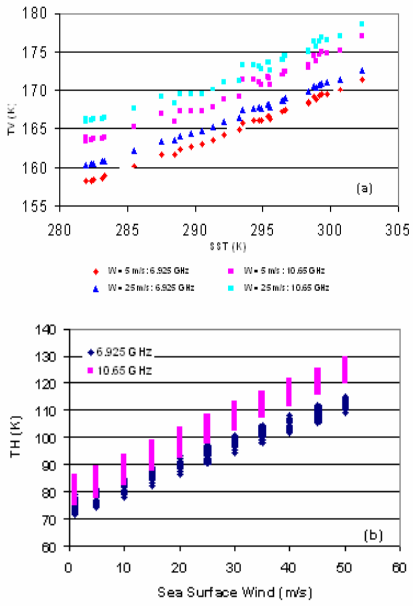

Figure 2. Simulated T_V (T_H) at 6.925 and 10.65 GHz as a function of SST (SSW) for various atmospheric profiles. (a) T_V vs. SST, when SSW of 5 and 25 m/s, respectively. (b) T_H vs. SSW.

3. ALGORITHM DESCRIPTIONS

3.1 AMSR-E Cloud Algorithm

AMSR-E cloud algorithm is an extension of a previously-developed emission-based algorithm for cloud liquid water [Weng and Grody, 1994; Weng, et.a l., 2003]. It contains retrievals for rain water (L_R), cloud water (L_C) and total precipitable water (V), as expressed as follows:

$$L_R = A_{01}\,\mu\,[\,\ln(T_S - T_{VC10}) - A_{11}\ln(T_S - T_{VC23}) - A_{21}\,] \quad (1)$$
$$L_C = A_{02}\,\mu\,[\,\ln(T_S - T_{VC19}) - A_{12}\ln(T_S - T_{VC23}) - A_{22}\,] \quad (2)$$
$$V = B_0\,\mu\,[\,\ln(T_S - T_{VC37}) - B_1\ln(T_S - T_{VC23}) - B_2\,] \quad (3)$$

with

$$T_{VCf} = T_s[1 - \zeta_f^2(1-\varepsilon_{Vf})] \quad (4)$$

where T_s is the surface temperature (i.e., SST if measurements are over oceans), ε_V the emissivity at a vertical polarization, μ=cos θ where θ is the local zenith angle, the subscript 'f' the frequency.

The scaling factors of $A_{01}\mu$, $A_{02}\mu$ and $B_0\mu$ are function of cloud layer temperature t_c. The uncertainty in t_c obviously affects the performance of the cloud algorithm. For example, when t_c varies from 15 to 0 °C, the cloud liquid water scaling factor is reduced to 63 ~ 69% (depending frequency) of the cloud liquid water with t_c of 15 °C, as displayed in Fig. 3a, while the variation in water vapor scaling factor is relatively low (see Fig. 3b). This implies that the reliable information of cloud layer temperature plays a very important role especially in deriving accurate rain/cloud water.

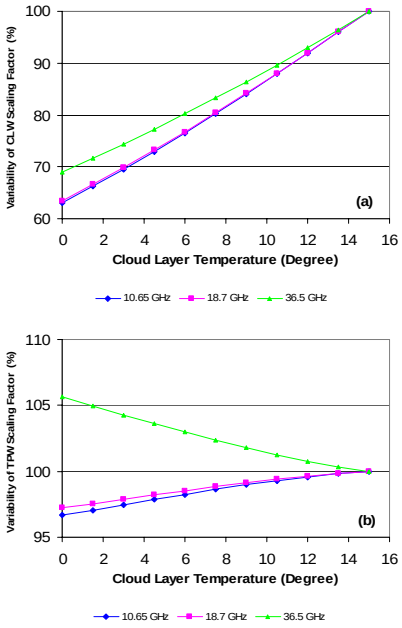

Figure 3. Variation of scaling factors (A and B) in Eqs. (1) – (3) due to cloud layer temperature at 10.65, 18.7 and 36.5 GHz for (a) cloud liquid water and (b) total precipitable water.

Note that in Eqs (1) to (3), the oceanic parameters regarding surface temperature and wind are also derived from AMSR-E data and their algorithms are discussed below.

3.2 AMSR-E Surface Algorithm

Emission-based radiative transfer equations in two polarizations are expressed as

$$T_{VS} = \varepsilon_V\zeta T_s + T_a + (1-\varepsilon_V)\zeta T_a \quad (5)$$
$$T_{HS} = \varepsilon_H\zeta T_s + T_a + (1-\varepsilon_H)\zeta T_a \quad (6)$$

The AMSR-E surface algorithm for sea surface temperature and wind is derived from Eqs. (5) and (6)

$$\begin{vmatrix} \Delta T_S \\ \Delta W \\ \Delta T_a \\ \Delta \zeta \end{vmatrix} = \left| (A^T A + E)^{-1} A^T \right| \begin{vmatrix} \Delta T_{V6} \\ \Delta T_{H6} \\ \Delta T_{V10} \\ \Delta T_{H10} \end{vmatrix} \quad (7)$$

where E is a matrix measuring the instrument noise and other sources of errors, and A is a matrix that is function of Ts, W, ζ and T_a.

4. RETRIEVAL RESULTS

4.1 Cloud and Rain Water Distributions

Figure 4a displays the distribution of the rain water derived from AMSR-E measurements at 10.65 and 23.8 GHz in November 8 of 2003, where Tc = T_s-8 (°K). A larger variability in rain water is detected over ocean region: its maximum is 2986 g/m^2 or 2.99 mm. This heaviest rain water is located in a band of heavy rainfall region to the south of Greenland and over Atlantic Ocean (see Fig. 4a). This result is consistent with rain rates derived from AMSU in NOAA operational Microwave Surface and Precipitation Products System (MSPPS).

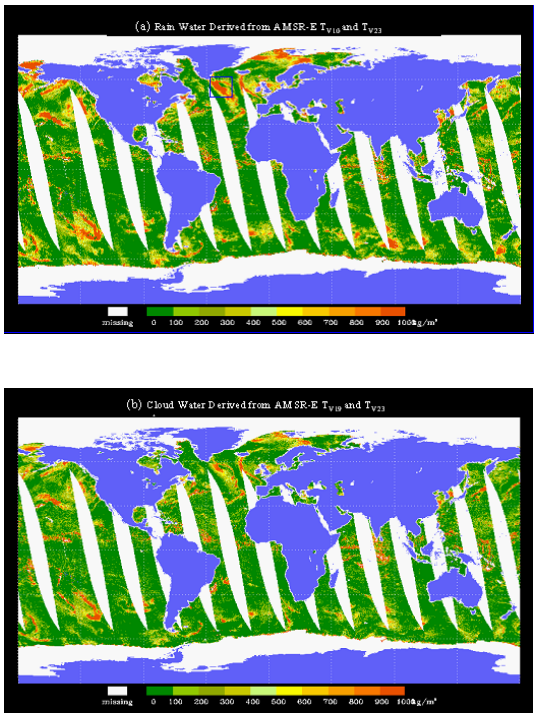

Figure 4. Distributions of rain and cloud water derived from AMSR-E measurements in November 8 of 2003. (a) Rain water. (b) Cloud water.

The cloud water derived from AMSR-E measurements at 18.7 and 23.8 GHz in Fig. 4b indicates a similar pattern to Fig. 4a, but its variability is limited to a relatively small dynamic range. The highest cloud water detected by this algorithm is 1.7 mm while it is an even smaller amount of 0.75 mm derived from 36.5 GHz. This is consistent with theoretical simulations in Figure 1: the higher the frequency, the lower the saturation value. It is noted that the cloud liquid water has been significantly underestimated especially using T_V at 36.5 GHz.

As part of the cloud algorithm, atmospheric total precipitable water is retrieved from AMSR-E measurements. Figures 5a shows the distribution of TPW derived from AMSR-E measurements. As a comparison, Figure 5b displays global distribution of TPW from GDAS product. It is found that a similar feature in TPW derived from AMSR-E to that of GDAS data over oceans.

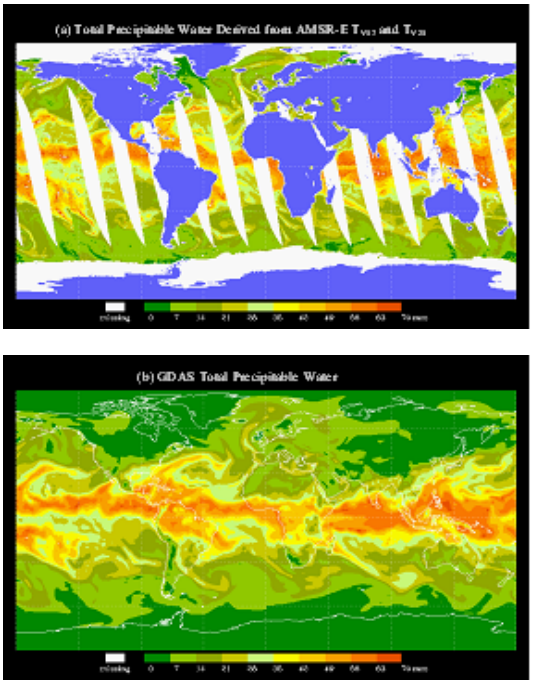

Figure 5. (a) Distribution of TPW in November 8 of 2003. (a) TPW derived from ascending AMSR-E measurements. (b) GDAS TPW.

4.2 SST and SSW Distributions

As discussed in section 3.2, in deriving AMSR-E surface algorithm for SST and SSW, an emission-based radiative transfer equation is utilized. In the presence of larger rain drops, there is a bias between brightness temperatures observed and simulated using Eqs. (5) and (6). To reduce the effect of this pure emission assumption, the satellite-measured brightness temperatures at 6.925 and 10.65 GHz are first adjusted

to modeled brightness temperatures for the SST and SSW retrievals using the following statistical relation:

$$T_{pS} = c_0 + c_1 T_{V6} + c_2 T_{H6} + c_3 T_{V10} + c_4 T_{H10} \quad (8)$$

where the 'p' denotes for either V- and H-polarization, and the coefficients $c_0 \sim c_4$ vary with each frequency and polarization. Compared to theoretically simulated brightness temperatures using Eqs. (5) and (6), T_{pS} produces an RMS error of about 0.6 °K and 0.8 °K at 6.925 and 10.65 GHz, respectively.

Performance of the AMSR-E surface algorithm is evaluated using simulated and observed brightness temperatures. Using simulated brightness temperatures at 6.925 and 10.65 GHz under various global atmospheric and ocean conditions (i.e., T_{VS} and T_{HS} have no error), the algorithm produces SST with a RMS error of 0.6 °K and SSW with a RMS error of 0.78 m/s. Furthermore, the performance of the algorithm is evaluated using AMSR-E measurements at 6.925 and 10.65 GHz against the SST and SSW data in NCEP GDAS and in National Data Buoy Center (NDBC), respectively. Results show that the corresponding RMS errors in SST and SSW are 1.6 °K and 1.7 m/s, respectively. Compared to simulated results, the increase RMS in SST and SSW is due to either the mis-match in time and space between AMSR-E measurements and NDBC data, or error in observed brightness temperatures. Figures 6a and 6b display distributions of SST and SSW produced using the AMSR-E surface algorithm A reasonable distribution is detected.

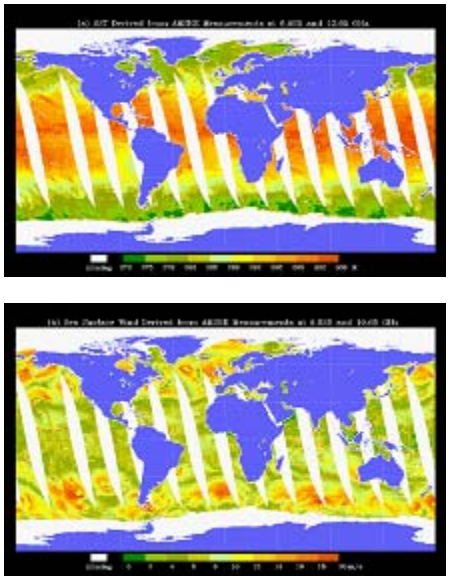

Figure 6. Distributions of SST and SSW derived from AMSR-E measurements in November 8 of 2003. (a) SST. (b) SSW.

5. DISCUSSION AND SUMMARY

The AMSR-E capability of deriving cloud, rain water, surface temperature and wind speed has been demonstrated through its lower frequency measurements. With the AMSR-E cloud algorithm, a large dynamic range in rain water is found using AMSR-E measurements at 10.65 and 23.8 GHz. As required in the cloud/rain water algorithms, an AMSR-E surface algorithm for SST and SSW is also developed. Its performance is evaluated against simulated and observed brightness temperatures with GDAS and NDBC SST and SSW data. An RMS error in SST and SSW is about 0.6 °K and 0.78 m/s, respectively, against simulated brightness temperatures, which basically represents the accuracy of the AMSR-E surface algorithm in the clear sky. Against observed brightness temperatures with GDAS and NDBC SST and SSW data, a mean RMS error in SST and SSW is increased to about 1.6 °K and 1.7 m/s, respectively, which primarily represents the accuracy of the AMSR-E surface algorithm in all weather conditions.

Acknowledgments: The views expressed in this publication are those of the authors and do not necessarily represent those of NOAA.

References

Weng. F., 1992: A multi-layer discrete-ordinate method for vector radiative transfer in a vertically-inhomogeneous, emitting and scattering atmosphere---I: Theory. J. Quant. Spectrose. Radiat. Transfer, **47**, 19-33.

Weng. F. and N. C. Grody, 1994: Retrieval of cloud liquid water using the special sensor microwave imager (SSM/I), J. Geophys. Res.,**99**, 25,535 -25, 551.

Weng. F., L. Zhao, R. R. Ferraro, G. Poe, X. Li., and N. Grody, 2003: Advanced microwave sounding unit cloud and precipitation algorithms, Radio Science, 38, Mar 33, 1-12.

Weng. F. and Q. Liu, 2003: Satellite data assimilation in numerical weather prediction models. Part I: Forward radiative transfer and jacobian modeling in cloudy atmospheres, J. Atmospheric Sciences, 2633-2646.

Wentz, F. J, 1997: A well-calibrated ocean algorithm for special sensor microwave /imager, J. Geophys. Res., 102, 8703-8718.